Supplementary Information for

Lewis-acidic Zr single-atom nanozyme with room-temperature glycosidase-like activity for cellulosic biomass degradation

Wenhua Zheng,[a] Fanxiang Meng,[b] Licong Zhao,[b] Fanye Zhang,[a] Ning Sui[a*]

[a]*College of Materials Science and Engineering, Qingdao University of Science and Technology, 53 Zhengzhou Road, Qingdao, Shandong 266042, China*

[b]*College of Chemical Engineering, Qingdao University of Science and Technology, 53 Zhengzhou Road, Qingdao, Shandong 266042, China*

Corresponding author

*E-mail: suining@qust.edu.cn

1. Materials and instruments

Zinc nitrate hexahydrate ($Zn(NO_3)_2·6H_2O$, 99%), 2-methylimidazole (99%), zirconium(IV) chloride ($ZrCl_4$, 99%), *N,N*-dimethylformamide (DMF, ≥99%), and methyl alcohol (CH_3OH, 99%) were purchased from Sinopharm Chemical Reagent Co., Ltd. (China). Nitrophenyl-β-D-glucopyranoside (PNPG, 98%), 3,5-dinitrosalicylic acid ($C_7H_4N_2O_7$, ≥98%), D-(+)-Glucose ($C_6H_{12}O_6$, ≥99.5%), potassium sodium tartrate tetrahydrate ($C_4H_4O_6KNa·4H_2O$, ≥99%), and phenol (C_6H_6O, ≥99%) were provided by Aladdin Chemical Reagent Co., Ltd. (China). All chemicals and reagents were used as-received without any further purification. All aqueous solutions were prepared with ultrapure water (18.25 MΩ cm) supplied by a Milli-Q® system (USA). Corn stover powder purchased from Shandong Province, China, was air-dried, ground, passed through an 80-mesh sieve, and stored at room temperature.

The morphology of the single-atom material was characterized using a transmission electron microscope (TEM, 2000 FX, JEOL Ltd., Japan) and a field emission scanning electron microscope (FE-SEM, JSM-7500F, JEOL Ltd., Japan). Phase structure analysis was performed using an X-ray powder diffractometer (XRD, D-MAX 2500/PC, Rigaku Corporation, Japan) in continuous scanning mode over a 2θ range of 20° to 80° with a step rate of 10° min^{-1}. Elemental chemical state analysis was conducted using an Escalab TM 250XI X-ray photoelectron spectrometer (Thermo Fisher Scientific, Madison, USA), equipped with a monochromatic Al Kα source (hυ = 1486.7 eV), an exit angle of 45°, an analysis spot diameter of 500 μm, and binding energy calibrated against the C 1s reference peak (284.8 eV). Absorbance measurements were obtained using a UV–visible spectrophotometer (Cary 5000, Agilent Technologies, USA). High-angle annular dark-field scanning transmission electron microscopy (HAADF-STEM) images and energy-dispersive X-ray

spectroscopy (EDS) elemental distribution maps were acquired using a JEOL ARM-200 microscope (200 kV, JEOL Ltd., Japan) equipped with an aberration corrector. The K-edge X-ray absorption spectroscopy (XAS) of the samples, including the X-ray near-edge absorption structure (XANES) and extended X-ray absorption fine structure (EXAFS), was collected at the Shanghai Synchrotron Radiation Facility (SSRF). Raw XAFS data underwent standard processing including background subtraction, normalization, and Fourier transformation using Athena software. EXAFS χ(k) data were analyzed via least-squares curve fitting with Artemis software, where theoretical scattering amplitudes, phase shifts, and mean free paths of photoelectrons were calculated using the FEFF8 ab initio program. Material synthesis was performed by calcination in a tube furnace (GSL-1600X-S60, Shanghai Precision, China).

2. Density functional theory (DFT) calculations

Materials computational studies were performed using CP2K software (version 2023.2). CP2K input files were generated via Multiwfn software (version 3.8), with geometric structure optimization employing the DZVP-MOLOPT-SR-GTH basis set and the GTH-PBE potential function based on the Perdew-Burke-Ernzerhof (PBE) generalized functional. Van der Waals interactions were accounted for using Grimme's DFT-D3(BJ) method. A self-consistent continuous solvent model was employed to simulate the aqueous environment. All calculations were performed with a plane-wave energy cutoff of 400 eV. The convergence threshold for SCF iterations was set to 10^{-6}, and the Brillouin zone sampling employed a Γ-centered Monkhorst-Pack K-point grid. Transition state searches were performed using the dimer algorithm and CI-NEB method. Structure building and visualization were accomplished with VESTA software (version 3.5.8).[1] PDOS analysis and post-processing were conducted using Multiwfn.

The adsorption energy (E_{ads}) was defined as

where $E_{slab+adsorbate}$, E_{slab}, and $E_{adsorbate}$ denote the total energy of the adsorbed structure, the total energy of the slab surface, and the total energy of the separated adsorbate, respectively.

Supplementary figures and tables

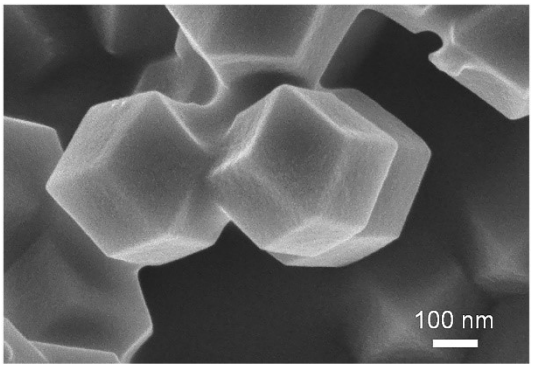

Fig. S1. SEM image of Zr-NC.

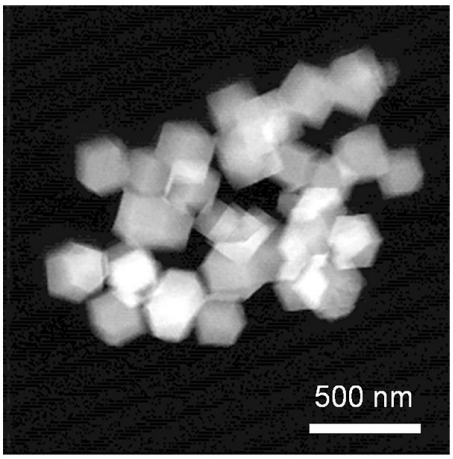

Fig. S2. Low-magnification STEM image of Zr-NC showing well-dispersed particles without noticeable aggregation.

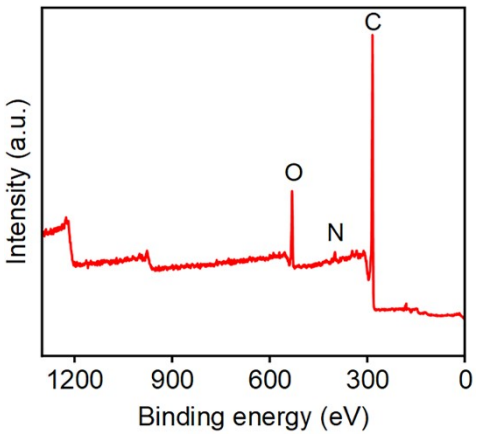

Fig. S3. XPS spectra for the Zr-NC survey scan.

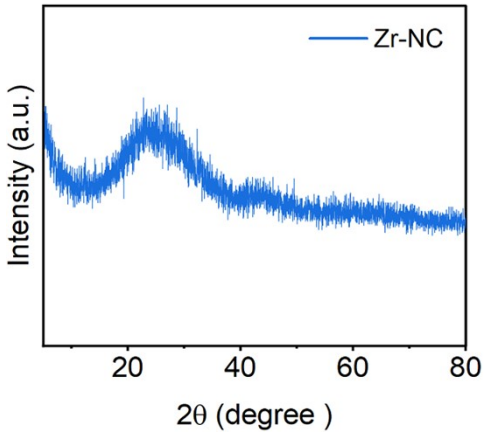

Fig. S4. XRD patterns of Zr-NC.

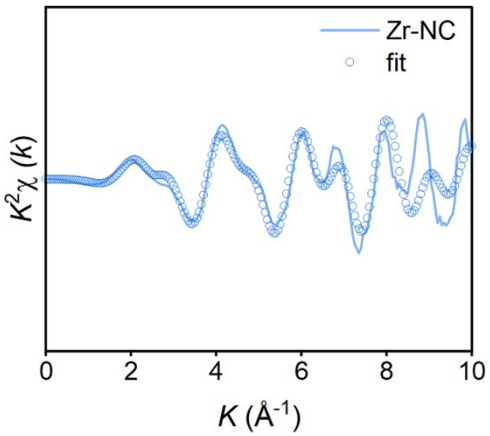

Fig. S5. EXAFS fitting results of Zr-NC in K space.

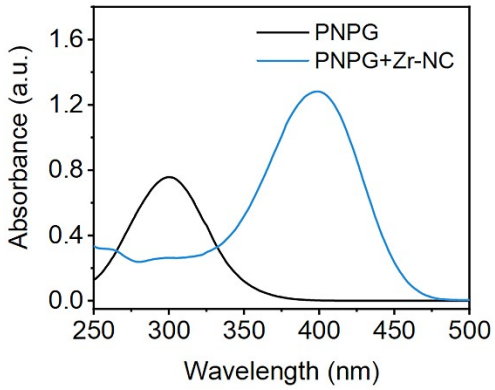

Fig. S6. UV-vis absorption spectra of the PNPG system and the PNPG + Zr-NC system at pH 5 and 25 °C. The concentrations of PNPG and Zr-NC were 1 mM and 100 μg mL^{-1}, respectively.

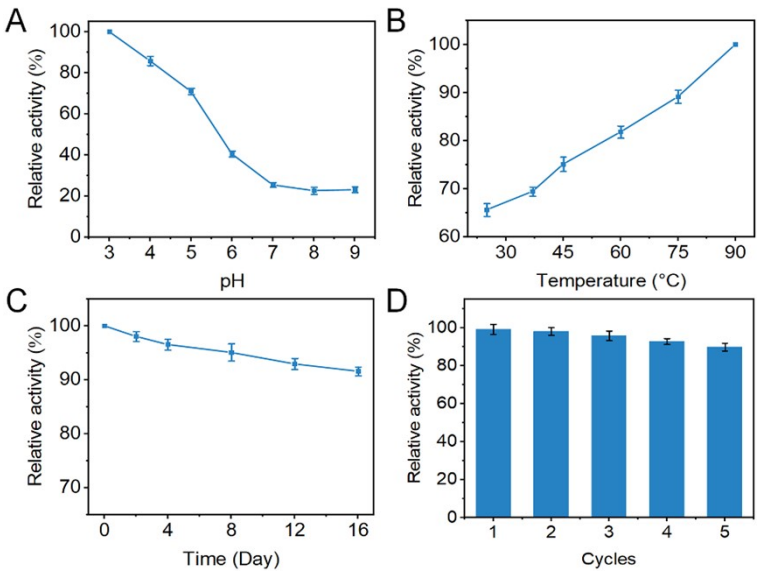

Fig. S7. (A) Relative activity of Zr-NC for PNPG hydrolysis at different pH values at 25 °C. (B) Relative activity of Zr-NC for PNPG hydrolysis at different temperatures at pH 5. (C) Relative activity of Zr-NC for PNPG hydrolysis as a function of reaction time at pH 5 and 25 °C. (D) Relative activity of Zr-NC for PNPG hydrolysis over different catalytic cycles at pH 5 and 25 °C. Reaction conditions: Zr-NC, 100 μg mL^{-1}; PNPG, 1 mM; reaction time, 10 min for (A), (B), and (D).

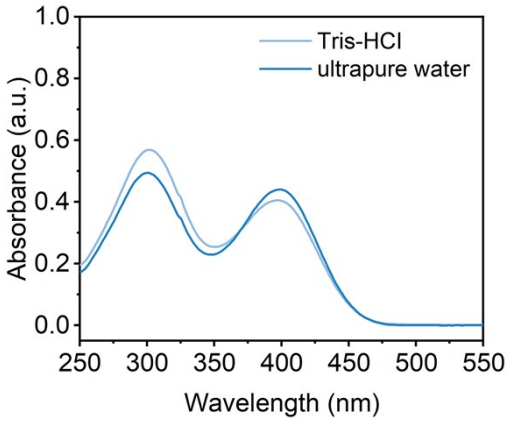

Fig. S8. UV-vis absorption spectra of PNPG hydrolysis catalyzed by Zr-NC in Tris-HCl buffer (pH 7) and in ultrapure water at 25 °C. Reaction conditions: PNPG, 1 mM; Zr-NC, 100 μg mL^{-1}; reaction time, 10 min.

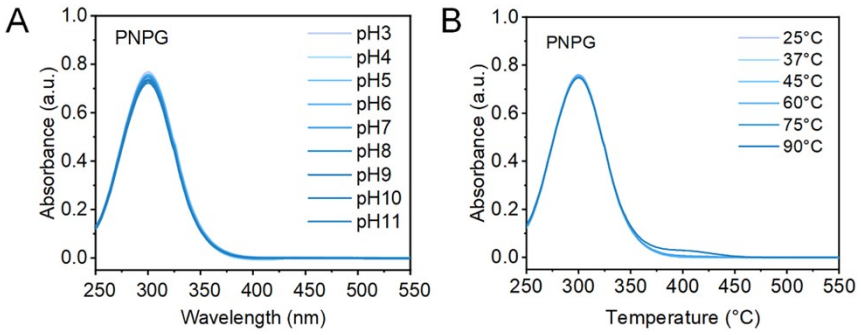

Fig. S9. Blank control experiments showing the UV–vis absorbance of PNPG in the absence of catalyst under different (A) pH values and (B) temperatures. (A) UV-vis absorbance of PNPG at different pH values at 25 °C. (B) UV-vis absorbance of PNPG at different temperatures at pH 5. Reaction conditions: PNPG, 1 mM; reaction time, 10 min.

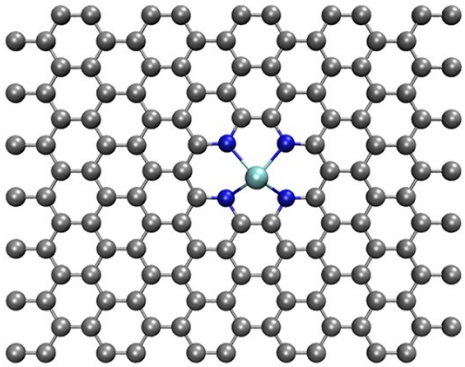

Fig. S10. Top views of Zr-NC obtained through theoretical calculations.

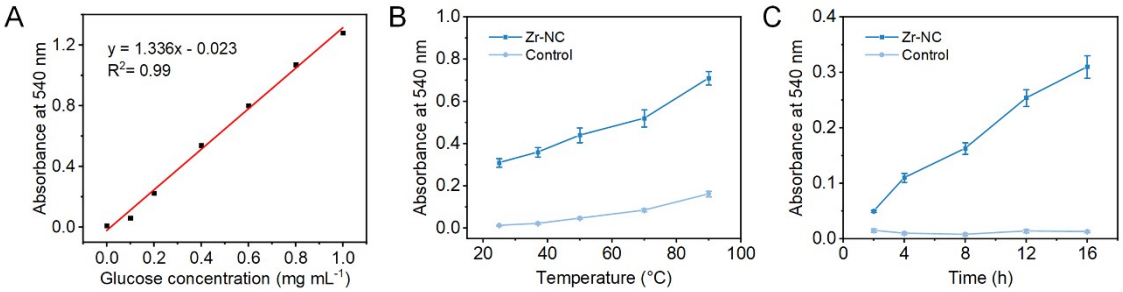

Fig. S11. (A) Calibration curve of D-glucose determined by the DNS assay based on the absorbance at 540 nm in ultrapure water at 25 °C. (B) Absorbance at 540 nm of the reaction supernatants, determined by the DNS assay, after treatment of corn stover powder with Zr-NC in ultrapure water at different temperatures for 16 h. (C) Absorbance at 540 nm of the reaction supernatants, determined by the DNS assay, after treatment of corn stover powder with Zr-NC in ultrapure water at 25 °C for different reaction times. Reaction conditions: Zr-NC, 100 μg mL^{-1}; corn stover powder, 2 mg mL^{-1}.

Table S1. EXAFS fitting parameters at the Zr K-edge for the samples (S_0^2 was fixed at 0.73, as derived from the Zr foil).

Sample	Shell	CN	R (Å)	σ^2 (10^{-2} Å^2)	ΔE_0 (eV)	R-factor (%)
Zr foil	Zr−Zr	1.1	1.48	-	-	-
Zr-NC	Zr−N	3.8	1.51	0.026	-2.56	0.012

Table S2. Michaelis-Menten kinetics for PNPG hydrolysis: comparison with representative inorganic catalysts and natural glycosidases reported in the literature.

Sample	Reaction conditions	K_m (mM)	V_{max} (μM min^{-1})	Reference
Cu_2O NPs	37 °C, pH 4, 200 μg mL^{-1}	1.69	10.76	[2]
Zr-NC	25 °C, pH 5, 100 μg mL^{-1}	1.83	15.54	This work
β-GC (*A.niger*)	37 °C, pH 5, 200 μg mL^{-1}	0.45	22.01	[2]
β-GC (almonds)	37 °C, pH 5, 2 μg mL^{-1}	3.13	47.90	[2]

Reference

1. K. Momma and F. Izumi, *J. Appl. Crystallogr.*, 2011, **44**, 1272-1276.

2. Z. Yu, J. Chen, D. Chao, X. Sun, L. Liu and S. Dong, *App. Catal. B: Environ.*, 2023, **330**, 122639.